Geochemical Journal, Vol. 36, pp. 443 to 463, 2002

Behavior of the REEs and other trace elements during fluid-rock interaction related to ore-forming processes of the Yinshan transitional deposit in China

QI-CONG LING[1,2]* and CONG-QIANG LIU[1]

[1]Institute of Geochemistry, Chinese Academy of Sciences, Guiyang 550002, China
[2]China University of Geosciences, Wuhan 430074, China

(*Received June 29, 2001; Accepted April 3, 2002*)

REE and other trace elements in altered and unaltered phyllites, orebodies and quartz veins in the Yinshan deposit were determined in order to examine behaviors of trace elements during hydrothermal alteration. REE, especially LREE, were selectively leached from the phyllites that had been undergone recrystallization dominantly of the major minerals during hydrothermal alteration. The greater the degree of alteration was, the stronger the leaching of REE would be. LREE were leached from the rocks that are close to the intrusions and re-deposited in the part far away from the intrusions. Nevertheless, Eu was systematically leached from the rocks, resulting in strong negative Eu anomalies in the altered phyllites. The lower total REE contents in the altered rocks close to the intrusions, compared to those from the further part is probably attributed to the dilution of REE-barren minerals (quartz and sulfides), and the removement of REE from the rocks by hydrothermal alteration. REE in the hydrothermal solutions are characterized by enrichment in LREE, strong positive Eu anomalies and $(La/Yb)_N$ ratios much smaller than those of the phyllites. The addition of REE from the hydrothermal solutions into the altered rocks resulted in the observed smaller $(La/Yb)_N$ ratios in the altered phyllites than that of the unaltered equivalent. For other trace elements, Y behaved similarly to HREE. The LIL elements such as Rb, Sr and Ba behaved differently, which may be attributed to the different fates of their main hosting minerals. The ore-forming elements such as Cu, Pb, Zn, Ag and Sn were remarkably added to the altered phyllites, while Hf, Th, U, Nb, and Zr remained rather constantly during hydrothermal alteration. It is suggested by the REE features that ore-forming fluids probably found their ways upwards from the depth through faults to the locus of ore deposition. The degree of REE mobility increases with the sizes of the orebodies. Thus, REE is probably an effective geochemical indicator for distinguishing between small and large orebodies at the later stage of exploration.

INTRODUCTION

Most studies on geological behaviors of rare earth elements (REE) in hydrothermal environments have dealt with active systems, while relatively little work has been published on REE distribution in hydrothermal systems (Ling and Liu, 2001). Several authors (Giuliani *et al.*, 1987; Matthews *et al.*, 1996; Vander and Andre, 1991) find that little or no evidence of trace element mobility during the formation of skarns. Bau (1990) concludes that REE systematics in rocks are not significantly affected by hydrothermal or metamorphic fluid-rock interaction except where strongly fluid-dominated alteration or intense infiltration metasomatism has occurred. In contrast, Whitney and Olmsted (1998) notice that REE patterns of skarns are significantly different from those of their protolith, indicating that the REE are highly active during metasomatism. Terakado and Fujitani (1998) find that trace elements in the rock may display highly selective behaviors dur-

*Corresponding author (e-mail: qcling@ms.gyig.ac.cn)

ing hydrothermal alteration. Boulvais *et al*. (2000) notice that fluid-rock interaction had led to intensive activity of REE and other trace elements in marbles. All investigations mentioned above indicate that behavior of trace elements in hydrothermal systems is very complex, and thus more studies are necessary for a better understanding the REE behavior in hydrothermal system. In this study, we report REE and other trace element abundances in ores, intrusion and related wallrock for the Yinshan transitional deposit in eastern China, which are considered to have been formed in strong fluid-rock interaction related to ore-forming processes.

The Yinshan deposit is a super-large polymetallic Cu-Zn-Pb-Ag-Au deposit, belonging to a "transitional deposit" according to the definition of Panteley (1986) that refers to those special ore deposits located between porphyry copper deposits at the depth and epithermal deposits at shallow depth, and it is one of the largest transitional deposits so far found in China (Zhang, 1997; Zhang and Liu, 1999). It is characterized by developing "perfect" symmetric hydrothermal alteration zonation in the host phyllite around the intrusion in the center of the deposit, and the orebodies occur in the altered phyllite. Although the formation processes for hydrothermal alteration zones and orebodies in the Yinshan deposit are not completely understood, the following model is addressed (Jiangxi G.E.B., 1996; Zhang, 1997): (1) the multistage hydrothermal fluid ascended along cracks developed in the contact between intrusion and wallrock, and infiltrated laterally into the wallrock, causing hydrothermal alteration zonation around the intrusion; (2) at later stages the same source hydrothermal fluid mixed up with parts of the descended circulating strata water in depth that evolved into ore-forming fluid and ascended along the same way, by filling into fractures in the wallrock, the orebodies were formed. Thus, we studied the distributions of the REE in ores and the related rocks with different degrees of alteration, with a main purpose to obtain a better understanding of geochemistry, especially the mobility of the REE and other trace elements during water/rock interaction related to the ore formation, and finally to get some information on the relationship between the REE mobility and the mineralizing event.

Geological Setting

The Yinshan deposit is located in northeastern Jiangxi Province, eastern China (Fig. 1). In the area is primarily distributed the Middle Proterozoic Shuangqiaoshan Group, the sericite phyllite, a suite of low-grade metavolcano-sedimentary rocks, which are mostly composed of sericite, with minor amounts of quartz, muscovite and calcite. The Shuangqiaoshan Group has thickness up to 2500 m, strikes nearly E-W direction and dip northwards with a dipping angle of 66°–85°. The stratum is relatively homogenous in lithology.

Two types of intrusion have been recognized at the Yinshan area: they are dacite porphyry ($3^{\#}$) and quartz porphyry ($13^{\#}$) (Fig. 1). Both types occur as dyke-like intrusions and are considered to have been derived from the same deep magmatic chamber (Zhang, 1997).

Affected by magmatism, the Shuanqiaoshan Group phyllite within the mine area has been hydrothermally altered. The altered part of the phyllite can be classified into the following alteration zones: quartz-sericite zone, quartz-carbonate-kaolinite zone, chlorite zone in the order from the center (Nos. 3 and 13 intrusions) to the margin (Jiangxi G.E.B., 1996, Fig. 1a). The quartz-sericite zone is most developed, up to 500 m thick revealed by underground workings.

The Shuangqiaoshan Group sericite phyllite far away from the mine area has not been affected by magmatism. So we can get a better understanding of the REE behavior during hydrothermal alteration by comparing the REE and other trace element compositions of altered phyllites with those of these unaltered ones.

In the Yinshan mining district, faults and fractures are well developed in the Shuangqiaoshan Group. These faults and fractures extend mainly in NEE-EW, NW-NNW or NE-NNE directions,

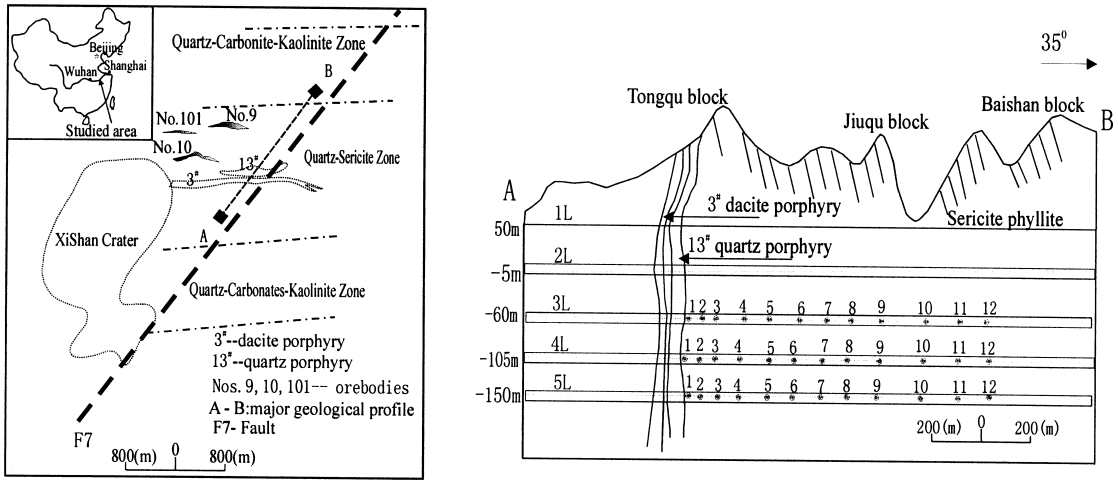

Fig. 1. (a) Geological sketch map of the Yinshan mining district, showing the alteration zones of phyllite and the spatial positions of intrusions and orebodies; (b) the distribution of samples in the main geological profile. 1L–5L are the underground workings being used for mining transportation.

with dipping angles of 70° to 90° and some of them extending to a depth of 1500 m. They are the main ore-controlling and orehosting structures (Jiangxi G.E.B., 1996).

The orebodies occur within the Shuangqiaoshan Group sericite phyllites. The major orebodies exist as veins, with a dipping angle of over 70°. They are a few tens of meters to several hundreds of meters long and a few meters to over ten of meters thick, and extend to over 1300 m in depth. Then the vein-type orebodies give way to the porphyry-type orebodies (Cu, Au) in depth. The orebodies are apparently controlled by faults and fractures, extending approximately parallel to the schistosity of the host rocks, several tens to several hundreds of meters apart from the intrusions. Generally there is no distinct boundary between orebodies and the host rock and the orebodies can only be defined in terms of their grades. In mineralogical assemblage, the ores are composed of quartz, galena, sphalerite, pyrite and variable amount of sericite. The contents of sulfides are negatively correlating with those of quartz. As deduced from their occurrence, both quartz and sulfides were probably precipitated from the same fluid system.

Based on O, H, C and Rb-Sr isotopic and fluid inclusion studies, and combination with comprehensive geological investigation, Jiangxi G.E.B. (1996) and Zhang (1997) proposed that the $3^{\#}$ and $13^{\#}$ intrusions are the center of hydrothermal alteration and mineralization in the Yinshan deposit. Alteration zonation is well developed from the contact outwards with the temperature changing from relatively high to low. The fractures developed in the contact between intrusions and phyllites serve the channel ways for the ascending of fluids, and then the fluids would penetrate and diffuse toward the host rocks, thereafter causing wallrock alteration. At the later stages the same source hydrothermal fluid mixed up with parts of the descended circulating strata water in depth, evolved into ore-forming fluid and ascended along the same way, by filling into fractures in the wallrock, the orebodies were formed. Therefore, the metallogenesis is closely related to fluid-rock interaction alteration in the mine area.

SAMPLING AND ANALYTICAL METHODS

Sample collection

Sampling was carried out systematically on three levels underground exposures (–60 m, –105 m and –150 m in Fig. 1). Along the main geologi-

Table 1(a). Hydrothermal altered phyllite on the 3rd level (–60 m) in the Yinshan deposit: major-element (wt.%), trace-element and REE (10^{-6}) abundances

	Away from the intrusion ←											Close to the intrusion
	3L12	3L11	3L10	3L9	3L8	3L7	3L6	3L5	3L4	3L3	3L2	3L1
Major elements												
SiO_2	47.75	51.96	52.62	55.56	55.88	59.87	60.58	60.94	61.57	62.22	64.45	66.85
TiO_2	0.52	0.3	0.25	0.3	0.45	0.32	0.38	0.15	0.62	0.36	0.40	0.51
Al_2O_3	17.51	20.31	19.9	19.64	18.90	17.71	19.73	19.84	16.77	16.38	16.74	16.06
[FeO]*	13.30	10.9	8.9	8.1	11.65	8.20	6.70	7.10	6.85	8.53	7.42	6.20
MnO	0.34	0.49	0.42	0.47	0.01	0.01	0.03	0.02	0.16	0.02	0.21	0.01
MgO	4.80	2.90	2.74	1.4	0.40	0.50	0.60	0.40	2.10	0.40	0.60	0.30
CaO	4.90	2.14	2.4	1.85	0.12	0.52	0.20	0.30	2.20	0.40	0.50	0.20
Na_2O	1.39	0.30	1.11	1.1	0.13	0.11	0.18	0.16	1.11	0.15	0.09	0.10
K_2O	1.00	4.17	4.18	4.5	4.43	5.20	5.1	4.86	3.84	4.31	4.29	4.19
P_2O_5	0.23	0.08	0.18	0.6	0.05	0.15	0.001	0.01	0.43	0.002	0.12	0.001
S*				2.2								
Ig. loss	7.69	5.92	6.98	4.07	7.41	6.72	5.98	5.80	3.79	6.87	4.50	4.90
Total	99.43	99.47	99.68	99.79	99.43	99.31	99.48	99.58	99.44	99.64	99.32	99.32
Trace elements												
Pb	230 (248)	650 (700)	250	50	140	24 (25)	5700 (6400)	110	34	67	220	49 (57)
Zn	800 (850)	2600 (2600)	770	140	110	200 (200)	5100 (5600)	310	41	47	340	200 (200)
Cu	83 (85)	64 (76)	58	92	460	22 (26)	74 (82)	270	260	850	1100	130 (140)
Ag	1.2 (0.95)	3.7 (3.39)	2.4	0.6	2.0	0.5 (0.46)	15.5 (18.17)	3.7	1.9	6.5	2.6	0.6 (0.59)
Rb	130 (130)	120 (120)	190	160	180	96 (91)	69 (71)	150	190	130	170	40 (40)
Sr	200 (230)	90 (110)	110	87	170	93 (100)	81 (98)	270	180	130	350	280 (320)
Ba	620 (600)	470 (510)	660	730	300	340 (330)	260 (280)	1100	590	520	570	140 (130)
Y	30 (31)	28 (32)	41	33	23	17 (16)	16 (17)	26	16	14	28	36 (34)
Zr	210 (220)	200 (200)	300	230	200	210 (210)	220 (230)	200	250	150	210	210 (220)
Nb	13 (13.41)	11 (12.80)	18	12	15	8.0 (8.10)	5.3 (6.01)	9.1	11	8.7	10	3.2 (3.30)
Hf	7.2 (7.10)	6.4 (7.07)	9.5	7.2	6.1	3.7 (3.24)	3.8 (3.88)	6.3	8.5	4.8	6.9	3.8 (3.69)
Th	13 (13.48)	9.6 (10.87)	14	11	11	8.2 (8.65)	5.3 (5.93)	9.4	13	10	9.7	2.2 (2.33)
U	2.3 (2.42)	1.8 (2.21)	2.8	2.3	4.6	0.86 (0.88)	1.2 (1.37)	3.4	4.3	3.4	3.9	0.6 (0.58)
Rare earth elements												
La	54.9 (56.4)	42.0 (46.5)	45.5	42.7	44.3	38.4 (37.3)	34.9 (36.5)	33.0	33.3	29.3	23.5	12.6 (12.2)
Ce	121 (125)	90.8 (98.9)	98.4	91.6	86.1	81.2 (80.2)	75.4 (80.0)	67.8	68.0	63.5	48.9	29.1 (29.6)
Pr	12.6 (12.87)	9.66 (10.64)	10.75	10.10	9.00	8.64 (8.48)	8.76 (9.39)	7.85	7.71	7.54	5.59	3.87 (3.93)
Nd	48.4 (48.5)	39.5 (41.2)	41.6	40.9	32.7	33.2 (32.5)	36.1 (37.4)	32.7	31.1	33.0	21.5	18.5 (18.6)
Sm	8.41 (9.12)	7.27 (8.34)	7.85	7.73	6.34	6.07 (6.15)	6.67 (7.56)	6.54	6.80	8.14	4.58	4.84 (5.14)
Eu	1.48 (1.48)	1.60 (1.86)	1.79	1.72	1.26	1.08 (1.12)	2.05 (2.31)	1.88	1.31	1.60	1.11	1.60 (1.67)
Gd	6.72 (6.86)	6.80 (7.41)	7.57	7.37	4.53	4.88 (4.51)	5.26 (5.46)	5.8	5.53	6.50	5.26	6.18 (6.04)
Tb	0.94 (0.99)	0.96 (1.06)	1.28	1.07	0.88	0.61 (0.60)	0.63 (0.69)	0.86	0.72	0.75	0.89	1.02 (1.00)
Dy	5.61 (5.67)	5.52 (6.01)	7.77	6.49	4.95	3.20 (3.22)	3.27 (3.35)	4.74	3.36	2.98	5.43	6.77 (6.68)
Ho	1.14 (1.19)	1.09 (1.17)	1.61	1.30	1.21	0.62 (0.61)	0.62 (0.61)	0.94	0.61	0.52	1.02	1.39 (1.38)
Er	3.47 (3.50)	3.23 (3.45)	4.74	3.61	3.44	1.90 (1.77)	1.62 (1.78)	2.97	1.94	1.65	3.48	3.90 (3.89)
Tm	0.50 (0.53)	0.45 (0.50)	0.69	0.55	0.45	0.27 (0.28)	0.27 (0.26)	0.44	0.32	0.30	0.50	0.59 (0.57)
Yb	3.88 (3.83)	3.54 (3.76)	5.32	3.82	2.89	2.96 (2.83)	1.82 (1.84)	3.36	2.63	2.39	3.48	3.83 (3.67)
Lu	0.55 (0.56)	0.48 (0.55)	0.72	0.53	0.42	0.27 (0.27)	0.27 (0.27)	0.5	0.44	0.34	0.49	0.56 (0.49)
ΣREE	270 (276)	213 (231)	236	220	199	183 (180)	178 (187)	169	164	159	126	94.7 (94.9)
Eu/Eu*	0.60	0.69	0.71	0.70	0.72	0.61	1.06	0.93	0.65	0.67	0.69	0.89
$(La/Yb)_N$	9.53	8.00	5.77	7.55	10.34	8.75	12.95	6.62	8.52	8.28	4.55	2.21
$(La/Sm)_N$	4.11	3.64	3.65	3.48	4.40	3.98	3.29	3.17	3.08	2.27	3.22	1.63

[FeO] = total Fe(Fe_2O_3 + FeO); S* = total S, no correction applied for O = S, ( ) = duplicate.*

cal profile (Fig. 1b A–B), samples were collected in the order from intrusions outwards, with intervals of 4–5 m where close to the intrusions and of 10–20 m in distal locations from the intrusions. The aim of such sampling was to sample phyllite representatively of various degrees of alteration. At the fourth level (–105 m), 300–400 m away from the intrusions, three orebodies with differ-

Table 1(b). Hydrothermal altered phyllite on the 4th level (–105 m) in the Yinshan deposit: major-element (wt.%), trace-element and REE (10^{-6}) abundances

	Away from the intrusion ←											Close to the intrusion
	4L12	4L11	4L10	4L9	4L8	4L7	4L6	4L5	4L4	4L3	4L2	4L1
Major elements												
SiO_2	49.99	52.3	51.94	52.92	53.42	58.23	58.75	61.53	60.06	61.74	62.46	63.94
TiO_2	0.35	0.36	0.48	0.22	0.42	0.32	0.13	0.12	0.37	0.72	0.16	0.001
Al_2O_3	18.42	18.67	14.40	17.24	17.30	18.19	19.37	19.39	17.05	15.82	16.53	19.37
[FeO]*	12.7	11.1	6.20	8.10	8.40	6.70	7.77	8.20	8.40	8.30	4.70	6.00
MnO	0.21	0.21	0.20	0.21	0.47	0.28	0.21	0.11	0.68	0.54	0.25	0.01
MgO	2.2	3.12	4.90	5.10	5.12	2.00	2.61	1.12	2.30	1.10	1.60	0.40
CaO	2.61	2.47	7.90	2.70	1.90	0.40	0.21	0.10	0.60	0.30	1.20	0.40
Na_2O	1.46	1.67	3.50	2.93	0.51	1.59	0.18	0.08	1.10	0.09	2.60	0.07
K_2O	2.86	3.81	0.90	1.56	2.59	3.52	3.19	2.32	3.00	3.76	4.00	4.88
P_2O_5	0.43	0.02	0.67	0.12	0.11	0.37	0.001	0.002	0.80	0.13	0.57	0.15
S*												
Ig. loss	8.42	5.93	8.24	8.15	9.59	8.18	6.92	6.35	5.44	6.97	5.36	4.19
Total	99.65	99.66	99.33	99.25	99.83	99.78	99.34	99.32	99.80	99.47	99.43	99.41
Trace elements												
Pb	170	25	35	120	120	21	35	64	67	6600	5800	24
Zn	1600	8400	730	3800	3700	490	1200	11000	200	8700	7300	87
Cu	92	5800	4800	11000	78000	470	5500	45000	32	96	88	89
Ag	2.1	4.3	4.5	84	35	1.6	2.1	150	0.64	8.5	10.3	1.2
Rb	120	220	180	170	120	200	150	110	140	140	110	36
Sr	190	52	32	33	320	27	24	28	120	45	130	300
Ba	510	610	520	540	550	1700	580	320	680	520	380	400
Y	36	45	35	17	13	34	35	14	31	25	32	21
Zr	220	220	230	210	220	220	230	220	220	210	210	220
Nb	14	13	12	12	8.6	13	12	8.0	11	9.2	10	6.4
Hf	6.8	8.2	7.0	6.9	5.8	7.0	6.7	6.7	6.8	6.7	5.4	3.5
Th	11	12	12	13	8.2	11	21	8.5	8.9	11	7.4	5.0
U	2.1	6.9	4.7	7.7	5.9	3.6	4.9	5.8	2.1	2.1	1.6	1.2
Rare earth elements												
La	50.0	45.1	41.3	38.2	37.6	37.3	37.2	30.4	29.0	26.0	23.6	17.4
Ce	106	90.0	84.0	81.6	81.3	77.3	75.2	64.5	62.6	56.0	52.6	37.7
Pr	11.3	10.7	9.74	9.09	9.30	8.70	8.02	7.46	7.15	6.38	6.04	4.43
Nd	42.6	44.1	38.5	37.2	37.6	35.8	29.7	28.1	27.8	24.8	25.9	17.7
Sm	7.85	9.29	8.71	7.65	7.30	7.00	5.95	6.02	5.77	5.23	5.44	4.00
Eu	1.72	2.64	2.38	2.11	1.83	1.37	1.51	1.35	1.34	1.20	1.36	0.85
Gd	7.57	9.75	8.73	6.61	5.54	6.23	5.93	4.12	5.75	4.85	6.34	4.37
Tb	1.09	1.49	1.21	0.8	0.69	1.00	1.03	0.60	0.91	0.78	1.00	0.68
Dy	6.56	8.47	6.56	3.6	2.75	5.98	6.16	3.42	5.77	4.54	5.70	4.05
Ho	1.34	1.60	1.29	0.63	0.54	1.26	1.30	0.78	1.17	0.89	1.19	0.77
Er	3.93	5.06	3.81	2.3	1.53	3.59	3.84	2.16	3.42	2.68	3.38	2.14
Tm	0.58	0.71	0.58	0.39	0.26	0.59	0.61	0.38	0.52	0.42	0.47	0.35
Yb	3.91	4.92	3.84	3.2	2.12	3.63	4.24	2.88	3.79	3.03	3.37	2.00
Lu	0.50	0.71	0.50	0.47	0.30	0.52	0.57	0.48	0.52	0.43	0.41	0.30
ΣREE	245	234	211	199	189	190	181	153	156	137	137	96.8
Eu/Eu*	0.68	0.85	0.83	0.91	0.88	0.63	0.78	0.83	0.71	0.73	0.71	0.62
$(La/Yb)_N$	8.61	6.18	7.25	8.05	12.0	6.92	5.92	7.12	5.15	5.79	4.73	5.85
$(La/Sm)_N$	4.00	3.05	2.98	3.14	3.24	3.35	3.93	3.18	3.16	3.13	2.73	2.74

[FeO] = total Fe(Fe_2O_3 + FeO); S* = total S, no correction applied for O = S.*

ent sizes were sampled (No. 10, 9 and 101 orebodies are measured at 10–15 m, 5–8 m and 1–2 m in thickness respectively). The host phyllites were sampled in the order from orebodies outwards, with the intervals of 1–2 m.

Unaltered phyllite samples were taken from the fresh surface outcrops of the Shuangqiaoshan Group along the Yinshan-Dexing Highway, about 20 km away from the Yinshan deposit, where phyllite is not believed to be affected by magmatic

Table 1(c). Hydrothermal altered phyllite on the 5th level (–150 m) in the Yinshan deposit: major-element (wt.%), trace-element and REE (10^{-6}) abundances

	Away from the intrusion ←											Close to the intrusion
	5L12	5L11	5L10	5L9	5L8	5L7	5L6	5L5	5L4	5L3	5L2	5L1
Major elements												
SiO_2	38.97	45.45	56.72	53.39	54.21	57.04	58.32	58.78	61.06	63.90	65.99	66.72
TiO_2	0.20	0.17	0.27	0.22	0.16	0.27	0.47	0.17	0.27	0.22	0.16	0.23
Al_2O_3	12.28	16.06	21.02	17.71	18.89	18.02	17.24	15.11	18.18	17.71	12.28	16.64
[FeO]*	23.00	17.10	8.50	10.80	11.90	9.70	9.80	9.20	4.80	5.60	6.60	3.70
MnO	0.07	0.04	0.20	0.26	0.03	0.05	0.41	0.91	0.09	0.02	0.01	0.03
MgO	0.52	0.50	2.21	2.20	0.50	0.70	1.90	1.60	0.70	0.30	0.20	0.10
CaO	0.40	0.20	0.50	0.40	0.10	0.10	0.40	0.50	0.40	0.10	0.10	0.21
Na_2O	0.70	0.90	0.90	1.01	0.90	1.10	0.90	1.00	1.00	1.00	0.50	0.90
K_2O	3.40	3.90	4.51	4.50	4.10	5.10	4.60	4.00	5.30	3.90	1.90	0.40
P_2O_5	0.80	0.73	0.47	0.40	0.97	0.57	0.50	0.63	0.70	0.60	0.67	0.62
S*	17.57	13.06			5.00				4.01	2.10	5.25	3.12
Ig. loss	1.50	1.20	3.98	8.90	2.67	6.98	4.92	7.60	2.98	3.85	5.62	6.51
Total	99.41	99.31	99.28	99.79	99.43	99.63	99.46	99.50	99.49	99.30	99.28	99.18
Trace elements												
Pb	84	950	46	1300	56	28	130	70	66	240	1600	350
Zn	180	410	200	8600	140	160	350	390	110	94	4900	16
Cu	630	2100	2300	170	410	170	2200	520	1300	1200	1700	94
Ag	2.1	24	1.6	83	15	5.4	2.1	0.64	150	160	157	65
Rb	190	130	140	130	200	180	190	220	140	77	190	14
Sr	58	190	38	80	86	41	180	75	58	1400	82	660
Ba	510	770	290	490	590	610	880	600	340	320	1100	200
Y	46	40	7.9	28	65	30	37	33	14	11	8.4	9.3
Zr	240	220	230	230	220	230	220	220	210	230	230	230
Nb	13	10	12	10	12	13	8.9	12	9.4	12	8.1	13
Hf	8.6	12	5.2	6.3	7.2	7.3	5.6	7.2	7.8	7.4	2.8	7.8
Th	15	8.7	9.2	11	10	9.4	8.2	11	7.7	10	8.2	8.3
U	4.1	3.5	4.0	2.4	5.5	2.7	3.5	2.7	3.7	3.7	6.4	2.9
Rare earth elements												
La	47.1	39.0	40.3	33.7	28.7	32.6	26.9	24.0	24.2	20.7	22.9	17.6
Ce	100	86.6	86.0	71.4	57.9	68.9	59.6	51.0	49.6	42.9	40.8	35.4
Pr	11.4	9.98	9.04	7.39	6.70	7.42	7.22	5.80	5.76	4.87	4.31	4.38
Nd	46.3	39.2	33.8	30.7	27.0	29.7	29.2	23.4	22.5	19.4	14.1	15.5
Sm	9.14	8.27	6.12	6.29	5.98	5.67	6.44	5.18	4.49	4.48	2.76	3.43
Eu	2.22	2.15	1.58	1.59	1.85	1.25	1.66	1.45	1.14	1.04	0.74	0.67
Gd	8.55	6.23	5.44	5.87	7.78	5.13	5.79	5.19	3.90	4.77	3.12	2.98
Tb	1.52	0.94	0.54	0.92	1.49	0.83	0.95	1.02	0.55	0.48	0.41	0.38
Dy	8.30	6.56	2.05	5.37	10.91	5.27	6.61	5.93	2.81	2.39	1.64	1.61
Ho	1.72	1.57	0.35	1.10	2.56	1.13	1.42	1.25	0.57	0.47	0.36	0.36
Er	4.77	4.35	0.90	3.12	7.08	3.33	4.11	3.53	1.76	1.44	1.12	1.19
Tm	0.68	0.66	0.16	0.46	1.02	0.54	0.60	0.57	0.31	0.26	0.22	0.23
Yb	4.72	4.39	4.10	3.72	2.35	3.93	3.75	3.80	2.48	2.11	2.36	2.12
Lu	0.68	0.60	0.17	0.55	0.80	0.57	0.51	0.55	0.40	0.35	0.42	0.38
ΣREE	247	210	191	172	162	166	155	133	121	106	95.2	86.3
Eu/Eu*	0.77	0.92	0.84	0.80	0.83	0.71	0.83	0.86	0.83	0.69	0.77	0.64
$(La/Yb)_N$	6.73	5.99	6.63	6.10	8.25	5.60	4.83	4.26	6.58	6.62	6.53	5.60
$(La/Sm)_N$	3.24	2.97	4.14	3.37	3.02	3.62	2.62	2.92	3.39	2.91	5.21	3.23

[FeO] = total Fe(Fe_2O_3 + FeO); S* = total S, no correction applied for O = S.*

activities.

Each specimen was prepared by mixing 3–4 rock samples collected from the same location in order to obtain representative data.

Analytical methods

All samples were crushed and ground manually. The selected specimens were first crushed by using a steel mortar and then ground to less than

–200 mesh powder by using an agate mortar. Major elements were determined by the wet chemical method. The sample powders were sealed in a Teflon bomb and digested in hydrofluoric and nitric acid (1:1). REE and other trace elements were analyzed by ICP-MS with a precision being better than 7% for REE and 10% for other trace elements. For low-concentration sample (quartz), trace elements were pre-enriched by increasing the quantity of digested sample and diminishing the volume of titrant. The published paper (Qi *et al*., 2000) can be referred to for the details of the analytical procedure. In the processes of analysis, the international standards AMH-1 and OU-3 were used as standard samples for quality controls. Duplicate determination for five representative samples gave results consistent within the limit of errors (Table 1). Some of the samples were used for duplicate analysis by X-ray fluorescence spectrometer for Zr contents. The major elements, REE and other trace elements were determined at the Open Lab. of Ore Deposit Geochemistry, Institute of Geochemistry, Chinese Academy of Sciences. Mineral assemblages and artificially panned minerals in the phyllites were analyzed by the optical methods in combination with X-ray (powder) diffraction analysis at the Center of Analysis and Test, China University of Geosciences.

RESULTS

Wallrock of the intrusions

Major elements The major element, together with REE and other trace element analyses for altered phyllite on the three levels of the main geological profile are shown in Table 1. Only those elements that can be accommodated in the structures of sericite, quartz, pyrite and calcite are present in significant concentrations in altered phyllites around the intrusions. By comparison with the unaltered phyllite (Table 3), variation trend of major elements in altered phyllites on the three levels are basically consistent. SiO_2 contents of the altered phyllites, e.g., on the 3 rd level, ranging from 66.85 to 47.75, increasing gradually from the outer part of the alteration zone to the rocks

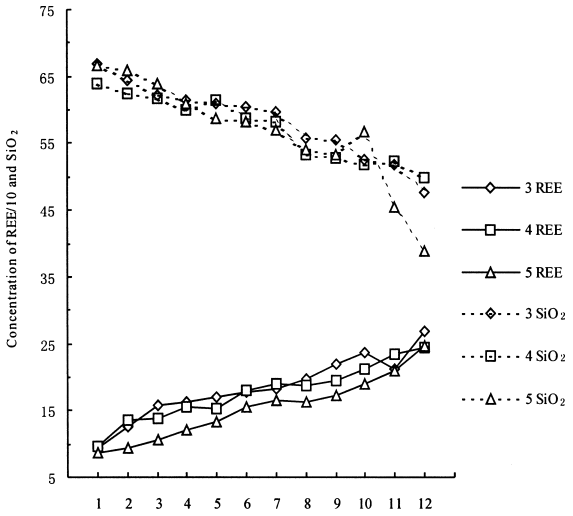

Fig. 2. Variation tendency of SiO_2 and REE in the altered wallrocks of the intrusions. 3, 4, 5 stand for 3L, 4L and 5L respectively; REE: the total REE content.

close to the intrusions (Table 1 and Fig. 2). This is consistent with the fact that a large number of micrometer-scale (3–8 μm) quartz or quartz + sulfide (e.g., pyrite, sphalerite, galena, etc.) stringers can be observed in samples that close to the intrusions. Meanwhile, scattered quartz grains in phyllite in the zone close to the contact is much larger than those in the zone far away from the intrusions. Some of the samples collected from locations far away from the intrusion, e.g., samples 3L10 $\rightarrow$ 3L12, 4L9 $\rightarrow$ 4L12 and 5L11 $\rightarrow$ 5L12, have Si contents even lower than that of the average unaltered phyllite. These samples have higher Ca or Fe contents (these are probably related to carbonatization or pyritization). Al, K and Na contents remained rather constant in most samples, which may be related to the fact that all these elements are present largely in sericite and that the sericite has undergone only recrystallization during hydrothermal alteration. Fe contents of altered phyllites are generally much higher than that of the unaltered phyllite, which can be interpreted by the observed extensive development of pyritization. Ti and P contents are very low and remained rather constant, but little is known about its forms of occurrence. The loss on ignition for

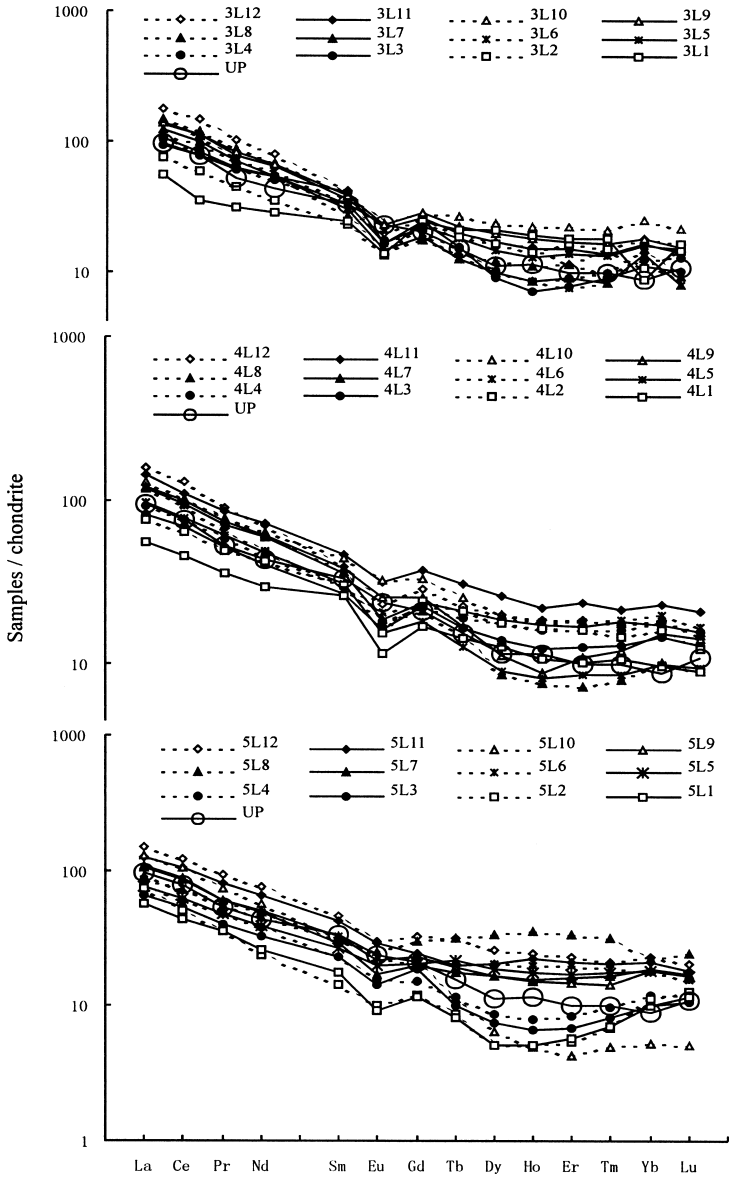

Fig. 3. Chondrite-normalized REE patterns of the altered and unaltered phyllites on the three levels.

altered phyllites is generally higher than that of the unaltered phyllite owing to the hydrothermal alteration.

REE and other trace elements REE contents in altered phyllites on the three levels in the main geological profile show the following features. The first, though somewhat variable contents of each element in different samples, the shapes of the chondrite-normalized REE patterns of the altered phyllites are quite similar to that of the unaltered phyllite, i.e., enrichments of light REE (LREE), negative Eu anomaly and relatively flat heavy REE (HREE) patterns (Fig. 3). Moreover, the total REE amount ($\sum$REE) tends to increase apparently in samples from the contact of the intrusion outwards (samples 1 $\rightarrow$ 12 in Fig. 2). Ex-

cept for samples from the locations where are very close to the contact (samples 3L1, 3L2; 4L1 to 4L3; and 5L1 to 5L5 in Table 1) that have lower ∑REE, the altered phyllite samples have higher ∑REE than that of the average unaltered phyllite, with a maximum enhancement up to 80.2%. The second, the enrichment of LREE over HREE, expressed as the chondrite-normalized ratio $(La/Yb)_N$, ranges from 2.21 to 10.34 in the altered samples, and is lower than that of the unaltered phyllite (10.93), excepting for samples 36 and 48. This is particularly true for those samples near the contact. However, fractionation among LREE expressed as ratio $(La/Sm)_N$ show little variable. The third, most of the altered phyllite samples show stronger negative Eu anomalies than the unaltered phyllite, with Eu/Eu* ratios ranging from 0.61 to 0.89, lower than that of the unaltered phyllite (0.90) excepting for samples 3L5, 3L6, 4L9 and 5L11.

For other trace elements, large-ion lithophile (LIL) elements, such as Rb, Sr and Ba show very different features, Rb and Sr remain rather constant, while Ba contents of the altered rocks are generally higher compared to the unaltered equivalent. The ore-forming elements, such as Pb, Zn, Cu, Ag, and Sn in most of the altered phyllite samples are much higher than the average content in the unaltered phyllite, but their variations show no evident regularity in space. The high field-strength (HFS) elements Hf, Nb and Zr, as well as Th, U remain considerably constant.

Ores, quartz, intrusions and wallrock of the orebodies

The major element, REE and other trace element analyses for altered phyllite around the representative orebodies (Nos. 9, 10, 101) are listed in Table 2, and that for the altered and unaltered quartz porphyry, ores, quartz both in orebodies and in wallrocks are listed in Table 3.

The characteristics of the major elements and REE in wallrocks around the orebodies are generally similar to those in the main geological profile. It is particularly worth to note that Si contents decrease gradually away from the contact of the orebodies outwards to the outer part of the altered rocks (Fig. 4), showing chemical zonation around the orebodies. Meanwhile, REE in the rocks close to the orebodies are lower than those of the rocks far away from the orebodies (Fig. 4). It is clearly enough that the larger the size of orebody, the lower of REE contents in the altered phyllites around the orebodies (Table 2 and Fig. 4).

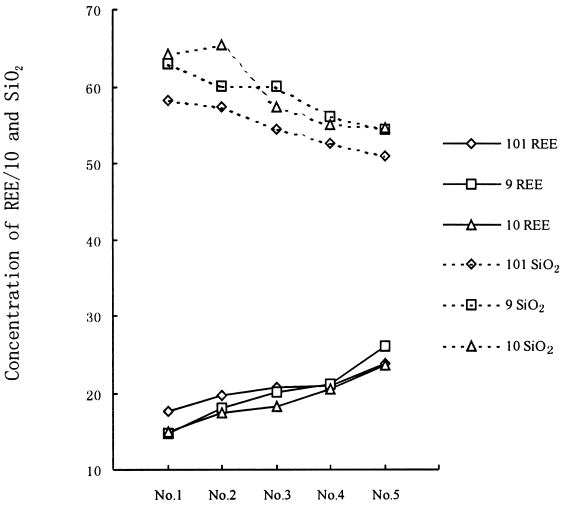

Fig. 4. Variation tendency of SiO_2 and REE in the altered wallrocks of the orebodies. 101, 9, 10 stand for Nos. 101, 9 and 10 orebody respectively; REE: total REE content. No. 1–No. 5 are the number of samples.

By comparison with the fresh quartz porphyry, the major elements of the altered samples (Table 3) are characterized by the decrease of Ca and Mg and the increase of Si and Fe in contents. This is consistent with the pervasive sericitization, silicification and pyritization. The sericitization removes Ca and Mg from the rocks, which can be described in the following reaction:

$$(Ca_2Na_2(Mg,Fe^{2+})_4(Al,Fe^{3+})[(Si,Al)_4O_{11}]_2(OH)_2 \text{ (hornblend)} \rightarrow K\{Al_2[AlSi_3O_{10}](OH)_2\} \text{ (sericite)}.$$

The silicification and pyritization add Si and Fe to the rock, as observed in the quartz porphyry. However, K, Na, Al, Ti, Mn, and P remain almost unchanged and the loss on ignition (including mainly H_2O and CO_2) is enhanced.

Table 2. Wall rocks of the representative orebodies in the Yinshan deposit : major-element (wt.%), trace-element and REE (10^{-6}) abundances

	1015	1014	1013	1012	1011	95	94	93
Major elements								
SiO_2	50.99	52.66	54.5	57.36	58.35	54.62	56.12	60.07
TiO_2	0.35	0.06	0.25	0.45	0.80	0.75	0.67	0.75
Al_2O_3	11.82	17.24	20.31	21.20	18.05	17.95	20.73	17.01
[FeO]*	15.70	14.72	6.704	9.10	9.80	10.00	7.10	8.40
MnO	0.01	0.02	0.51	0.20	0.47	0.31	0.15	1.62
MgO	0.20	0.40	1.10	2.20	2.40	2.40	1.60	2.30
CaO	0.10	0.10	0.40	0.20	0.70	0.50	0.20	0.70
Na_2O	0.06	0.10	0.11	0.70	1.10	1.00	1.00	1.00
K_2O	2.86	4.57	4.20	3.52	3.50	3.50	5.20	3.00
P_2O_5	0.63	0.25	0.01	0.57	0.40	0.73	0.33	0.58
S*						4.1		
Ig. loss	14.93	9.64	6.90	4.09	4.06	3.64	6.34	4.25
Total	97.65	99.76	94.90	99.59	99.63	99.5	99.44	99.68
Trace elements								
Pb	26	230	2900	2200	1100	2000	6800	490
Zn	220	510	4800	2700	940	3500	8800	2100
Cu	24	130	40	400	120	85	1700	90
Ag	0.49	2.0	6.0	5.3	89	140	9.0	1.5
Rb	100	190	180	160	160	150	160	230
Sr	100	69	120	69	50	49	75	73
Ba	370	650	480	570	420	470	670	820
Y	18	30	21	34	49	35	40	25
Zr	220	240	280	230	240	220	240	240
Nb	8.6	14	14	12	15	15	15	15
Hf	4.1	7.6	8.9	7.5	7.8	6.9	7.8	7.6
Th	8.9	12	13	13	15	13	14	17
U	0.94	2.6	2.7	2.4	3.0	2.7	3.1	3.9
Rare earth elements								
La	49.7	40.0	42.9	36.2	29.4	49.2	39.0	41.5
Ce	104	87.1	88.3	79.8	64.8	1098	84.8	88.0
Pr	11.2	9.68	9.98	9.15	8.15	12.3	9.90	9.67
Nd	43.0	39.3	39.2	37.3	33.1	50.0	40.0	36.6
Sm	7.85	7.88	7.50	7.44	8.13	10.45	7.88	6.67
Eu	1.64	1.68	1.70	1.76	1.98	2.09	1.74	1.38
Gd	6.68	6.96	5.31	7.79	8.37	8.23	7.66	4.70
Tb	0.79	1.01	0.71	1.22	1.45	1.23	1.26	0.68
Dy	4.13	5.54	3.82	6.97	8.76	6.95	7.35	3.93
Ho	0.81	1.11	0.83	1.40	1.81	1.34	1.52	0.89
Er	2.45	3.30	2.40	3.66	4.93	3.99	4.35	2.72
Tm	0.35	0.48	0.39	0.58	0.74	0.58	0.70	0.44
Yb	3.53	3.76	3.16	3.95	4.67	4.07	4.69	3.25
Lu	0.35	0.55	0.46	0.53	0.61	0.56	0.68	0.47
∑REE	237	208	207	198	177	260	212	201
Eu/Eu*	0.69	0.69	0.82	0.71	0.73	0.69	0.69	0.75
(La/Yb)	9.49	7.19	9.16	6.18	4.24	8.17	5.61	8.61
(La/Sm)	3.98	3.20	3.60	3.06	2.27	2.96	3.12	3.91

Table 2. (continued)

	92	91	105	104	103	102	101
Major elements							
SiO_2	60.01	62.97	54.76	55.14	57.37	65.50	64.21
TiO_2	0.72	0.31	0.25	0.32	0.35	0.16	0.27
Al_2O_3	16.29	15.11	17.01	20.25	19.10	17.95	19.84
[FeO]*	9.60	7.10	10.00	9.50	11.70	8.60	4.60
MnO	0.27	0.23	0.49	0.18	0.45	0.02	0.07
MgO	2.20	1.30	2.30	2.80	2.5	0.30	0.50
CaO	0.20	0.40	0.50	0.30	0.3	0.60	0.20
Na_2O	0.90	1.00	1.00	1.01	1.00	0.12	1.00
K_2O	3.30	3.20	3.70	3.80	3.20	3.67	4.80
P_2O_5	0.63	0.80	0.40	0.70	0.47	0.002	0.47
S*		1.01					
Ig. loss	5.64	5.99	9.30	5.70	3.37	2.70	3.6
Total	99.76	99.42	99.71	99.70	99.81	99.62	99.56
Trace elements							
Pb	280	1000	1400	2700	1700	80	700
Zn	2700	3100	1700	3600	1500	3.1	400
Cu	100	200	82	82	49	200	73
Ag	5.4	77	9.0	9.2	3.3	72	1.0
Rb	130	170	220	220	190	620	180
Sr	84	90	160	120	130	27	69
Ba	520	4400	630	650	420	350	660
Y	33	29	32	37	33	17	32
Zr	210	200	240	260	280	210	270
Nb	14	11	17	22	16	12	17
Hf	6.6	6.2	11	8.5	8.6	3.4	8.3
Th	10	9.0	17	15	14	12	11
U	2.0	2.2	3.6	3.3	3.0	3.2	2.5
Rare earth elements							
La	33.8	27.6	45.5	36.6	33.7	34.2	27.2
Ce	73.4	59.6	100.0	83.5	74.6	71.4	60.2
Pr	8.21	6.59	11.13	9.24	8.36	7.89	6.84
Nd	33.8	26.0	43.6	37.5	33.4	31.4	27.6
Sm	6.96	5.76	8.45	7.96	7.02	6.24	5.56
Eu	1.51	1.22	2.34	1.51	1.88	1.55	1.19
Gd	6.25	5.16	7.16	7.98	6.53	5.62	5.13
Tb	1.04	0.88	1.05	1.25	1.01	0.84	0.91
Dy	6.00	5.44	5.92	7.63	6.04	4.70	5.45
Ho	1.24	1.06	1.23	1.45	1.25	1.00	1.24
Er	3.57	3.25	3.96	4.19	3.66	3.23	3.58
Tm	0.58	0.51	0.59	0.60	0.56	0.53	0.60
Yb	3.82	3.20	4.24	4.86	4.22	4.17	4.17
Lu	0.53	0.44	0.64	0.66	0.59	0.66	0.61
∑REE	181	147	236	205	183	173	150
Eu/Eu*	0.70	0.68	0.92	0.58	0.85	0.80	0.68
(La/Yb)	5.97	5.80	7.24	5.08	5.38	5.52	4.41
(La/Sm)	3.06	3.01	3.39	2.89	3.02	3.45	3.08

[FeO] = total Fe(Fe_2O_3 + FeO); S* = total S, no correction applied for O = S.*

Table 3. Unaltered phyllite, altered and fresh rhyodacite, quartz in orebodies and wall rock in the Yinshan deposit: major-element (wt.%), trace-element and REE (10^{-6}) abundances

	UP (5)	AI (5)	UI (5)	101Ore(3)
Major elements				
SiO_2	58.89 (1.45)	63.41 (2.31)	61.51 (0.48)	46.55 (1.48)
TiO_2	0.66 (0.12)	0.32 (0.88)	0.46 (0.16)	0.80 (0.11)
Al_2O_3	16.86 (0.24)	14.02 (1.42)	15.20 (0.30)	12.04 (0.82)
[FeO]*	8.66 (0.35)	7.82 (0.81)	4.62 (0.38)	8.10 (1.56)
MnO	0.10 (0.02)	0.32 (0.02)	0.68 (0.03)	0.10 (0.02)
MgO	2.98 (0.35)	0.48 (0.35)	1.79 (0.44)	0.80 (0.36)
CaO	0.88 (0.07)	0.75 (0.21)	3.45 (0.09)	0.30 (0.21)
Na_2O	1.64 (0.05)	1.51 (0.39)	2.21 (0.07)	0.90 (0.38)
K_2O	4.34 (0.15)	3.42 (0.35)	4.22 (0.21)	2.50 (0.43)
P_2O_5	0.10 (0.06)	0.17 (0.06)	0.19 (0.07)	0.50 (0.05)
S*				7.18 (1.33)
Pb				12.47 (4.44)
Zn				2.22 (1.35)
Cu				0.63 (0.48)
Ig. loss	4.52 (0.58)	7.56 (1.44)	5.21 (0.02)	4.66 (0.46)
Total	99.63 (0.30)	99.78 (0.24)	99.53 (0.45)	99.75 (0.23)
Trace elements				
Pb	46 (4.11)	49 (4.30)	62 (5.22)	n.d.
Zn	140 (5.65)	120 (6.32)	140 (7.43)	n.d.
Cu	48 (2.30)	120 (4.10)	150 (6.12)	n.d.
Ag	0.1 (26.39)	2.0 (1.89)	2.2 (2.44)	35 (4.22)
Rb	140 (7.33)	180 (6.87)	190 (9.21)	120 (4.56)
Sr	240 (14.11)	170 (15.66)	140 (10.32)	320 (9.89)
Ba	390 (44.0)	300 (66.42)	680 (45.65)	550 (41.11)
Y	14 (3.10)	23 (9.23)	75 (2.43)	13 (1.12)
Zr	200 (16.62)	200 (23.46)	200 (20.11)	190 (0.99)
Nb	14 (0.08)	15 (1.12)	18 (0.09)	8.6 (0.07)
Hf	6.2 (1.55)	6.1 (1.46)	6.0 (1.22)	5.8 (0.98)
Th	10 (0.44)	11 (0.65)	11 (0.44)	8.2 (0.32)
U	4.0 (0.65)	4.6 (0.23)	14 (0.32)	5.9 (0.21)
Rare earth elements				
La	29.8 (1.33)	41.3 (1.47)	51.9 (1.12)	4.36 (1.34)
Ce	62.9 (13.62)	82.1 (9.54)	98.9 (7.43)	8.03 (1.23)
Pr	6.50 (0.35)	8.60 (0.39)	10.71 (0.41)	0.86 (0.31)
Nd	26.39 (1.03)	30.72 (1.04)	40.04 (1.89)	3.46 (1.22)
Sm	6.50 (0.25)	6.34 (0.32)	7.12 (0.21)	0.85 (0.42)
Eu	1.74 (0.01)	2.00 (0.02)	3.08 (0.02)	0.37 (0.06)
Gd	5.43 (0.84)	5.68 (0.86)	8.68 (0.99)	0.56 (0.67)
Tb	0.73 (0.07)	0.85 (0.08)	1.34 (0.04)	0.08 (0.03)
Dy	3.66 (0.56)	4.98 (0.77)	7.10 (0.46)	0.45 (0.43)
Ho	0.83 (0.10)	1.10 (0.22)	1.42 (0.44)	0.09 (0.42)
Er	2.07 (0.32)	3.21 (0.54)	3.65 (0.64)	0.28 (0.12)
Tm	0.32 (0.05)	0.61 (0.04)	0.66 (0.05)	0.05 (0.03)
Yb	1.84 (0.38)	3.66 (0.42)	3.50 (0.49)	0.42 (0.02)
Lu	0.36 (0.04)	0.54 (0.06)	0.46 (0.74)	0.06 (0.01)
∑REE	149	192	239	19.9
Eu/Eu*	0.90	1.02	1.20	1.64
$(La/Yb)_N$	10.93	7.61	10.00	7.00
$(La/Sm)_N$	2.89	4.10	4.59	3.23

Table 3. (continued)

	9Ore(3)	10Ore(3)	10Qz(3)	WQz(3)
Major elements				
SiO_2	5.64 (1.12)	5.96 (1.98)	n.d.	n.d.
TiO_2	0.02 (0.06)	0.06 (0.02)	n.d.	n.d.
Al_2O_3	0.66 (1.19)	0.09 (1.88)	n.d.	n.d.
[FeO]*	9.10 (0.98)	7.90 (0.87)	n.d.	n.d.
MnO	0.14 (0.03)	0.48 (0.02)	n.d.	n.d.
MgO	0.40 (0.66)	0.20 (0.43)	n.d.	n.d.
CaO	0.30 (0.33)	0.80 (0.41)	n.d.	n.d.
Na_2O	0.90 (0.77)	0.90 (0.56)	n.d.	n.d.
K_2O	0.10 (0.21)	0.30 (0.09)	n.d.	n.d.
P_2O_5	0.57 (0.06)	0.53 (0.08)	n.d.	n.d.
S*	20.99 (1.87)	21.85 (1.45)	n.d.	n.d.
Pb	3.60 (2.23)	2.70 (1.67)	n.d.	n.d.
Zn	53.50 (2.45)	47.40 (3.11)	n.d.	n.d.
Cu	0.25 (0.99)	0.25 (0.46)	n.d.	n.d.
Ig. loss	3.21 (0.12)	10.10 (0.32)	n.d.	n.d.
Total	99.36 (0.32)	99.52 (0.44)	n.d.	n.d.
Trace elements				
Pb	n.d.	n.d.	15 (2.21)	54 (1.98)
Zn	n.d.	n.d.	250 (11.11)	100 (0.89)
Cu	n.d.	n.d.	150 (1.23)	670 (2.01)
Ag	6.0 (1.98)	6.9 (1.88)	—	—
Rb	8.7 (1.23)	10 (0.98)	6.0 (2.23)	21 (2.12)
Sr	7.2 (0.44)	7.0 (0.34)	2.8 (0.34)	46 (0.67)
Ba	—	—	0.1 (0.12)	0.1 (0.12)
Y	20 (1.12)	21 (1.23)	0.4 (0.32)	5.7 (0.67)
Zr	99 (0.87)	100 (0.66)	0.9 (0.12)	1.4 (0.98)
Nb	11 (0.10)	10 (0.23)	0.6 (0.23)	0.2 (0.43)
Hf	6.2 (0.78)	6.7 (0.45)	0.1 (0.10)	0.04 (0.10)
Th	9.2 (0.31)	9.9 (0.12)	0.1 (0.05)	0.7 (0.10)
U	4.8 (0.34)	4.2 (0.23)	0.01 (0.01)	0.02 (0.10)
Rare earth elements				
La	0.75 (0.98)	1.46 (0.63)	0.64 (0.43)	2.12 (0.99)
Ce	1.43 (0.12)	2.73 (0.21)	1.12 (0.03)	2.94 (0.04)
Pr	0.16 (0.64)	0.28 (0.86)	0.11 (0.44)	0.26 (0.23)
Nd	0.65 (0.87)	1.12 (0.34)	0.42 (0.55)	1.06 (0.32)
Sm	0.17 (0.11)	0.36 (0.09)	0.12 (0.33)	0.36 (0.06)
Eu	0.14 (0.46)	0.37 (0.08)	0.08 (0.02)	0.31 (0.03)
Gd	0.21 (0.12)	0.64 (0.12)	0.10 (0.11)	0.62 (0.11)
Tb	0.03 (0.10)	0.10 (0.88)	0.02 (0.03)	0.08 (0.12)
Dy	0.13 (0.03)	0.54 (0.02)	0.13 (0.03)	0.52 (0.06)
Ho	0.03 (0.09)	0.10 (0.10)	0.03 (0.04)	0.11 (0.05)
Er	0.08 (0.11)	0.26 (0.32)	0.08 (0.02)	0.28 (0.03)
Tm	0.01 (0.04)	0.04 (0.01)	0.01 (0.01)	0.04 (0.01)
Yb	0.08 (0.02)	0.28 (0.03)	0.08 (0.02)	0.26 (0.06)
Lu	0.02 (0.02)	0.04 (0.03)	0.01 (0.03)	0.04 (0.01)
∑REE	3.90	8.30	3.00	9.00
Eu/Eu*	2.27	2.36	2.23	2.01
$(La/Yb)_N$	6.02	3.52	5.39	5.50
$(La/Sm)_N$	2.78	2.55	3.35	3.70

FeO] = total Fe(Fe_2O_3 + FeO); S* = total S, no correction applied for O = S; n.d.: not determined; —: under detected limit; UP: unaltered phyllite; AI: altered intrusion; UI: unaltered intrusion; 10Qz: quartz from 10 oredoby; WQz: quarz from wall rock.*

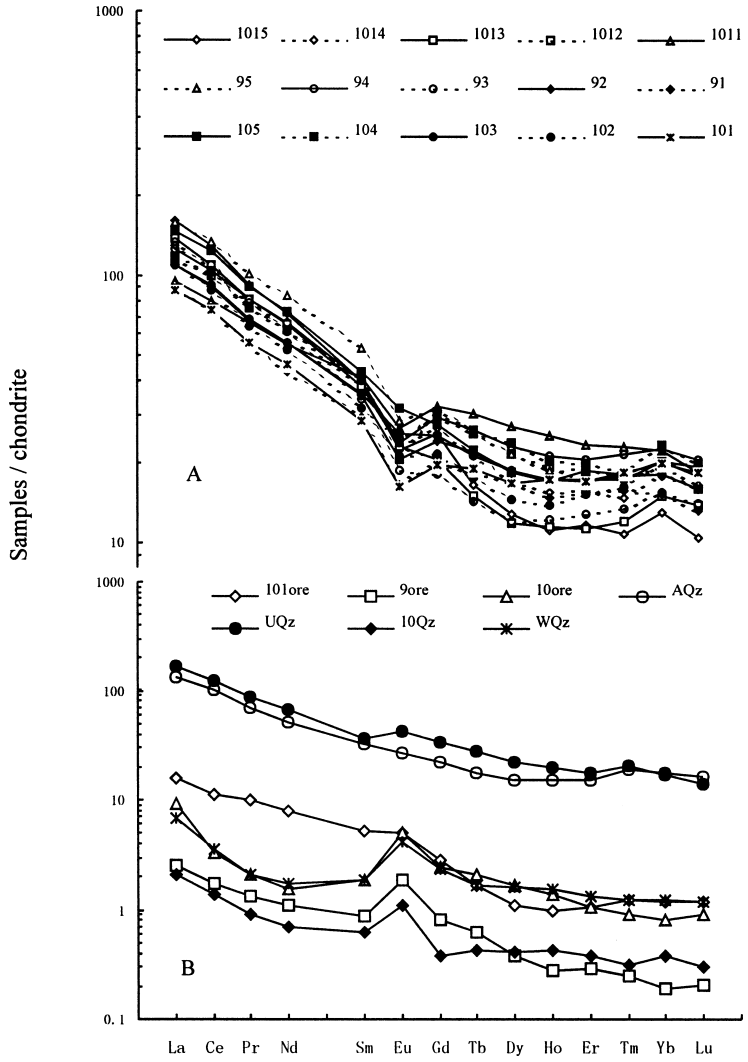

Fig. 5. Chondrite-normalized REE patterns of the altered wallrocks of the orebodies (A) and the intrusion, ores and quartz (B). AQz - altered quartz porphyry; UQz - unaltered quartz porphyry; 10Qz - quartz collected from No. 10 orebody; WQz - quartz collected from quartz vein in the wallrocks.

Except for the smaller Eu anomaly, the altered quartz porphyry has chondrite-normalized REE pattern very similar to that of fresh counterpart. Both of the altered and unaltered quartz porphyry are characterized with enrichment in LREE and slightly positive Eu anomalies (Fig. 5). Nevertheless, the total REE amount of the altered quartz porphyry is lower than that of the fresh equivalent. Moreover, the $(La/Yb)_N$ and Eu/Eu* ratios are also smaller than those observed in the fresh rocks. Accordingly, it is suggested that hydrothermal alteration removes REE, especially LREE and Eu from the quartz porphyry.

The chondrite-normalized REE patterns for the three representative orebodies are characterized by enrichment in LREE and very strong positive Eu anomalies with Eu/Eu* ratios ranging from 1.64 to 2.36. The $(La/Yb)_N$ ratios of the three orebodies are much lower than those of the wallrocks, while the $(La/Sm)_N$ ratios show little

difference. Their total REE amounts (∑REE) are significantly lower than those of the wallrocks. This may be related to the fact that the ores are composed mainly of sulfide such as pyrite, galena and sphalerite, which are commonly REE-barren minerals (Pan *et al*., 1993). Moreover, the three orebodies show some differences in ∑REE due to their differences in mineral assemblage: ore from the No. 101 orebody has relatively higher REE contents owing to the presence of higher REE-bearing sericite and other silicate minerals. Ores from the Nos. 9 and 10 orebodies have lower REE contents because they are made up predominantly of REE-barren minerals such as pyrite, galena and sphalerite.

Listed in Table 3 are also the results of chemical analysis of quartz, which are the monomineral samples of quartz that was hand-picked from ore-barren quartz veins in altered wallrock (WQz) and No. 10 orebody (10Qz) respectively. It is clearly that quartz either from the ore or from ore-barren quartz veins is characterized by very low ∑REE, with $(La/Yb)_N$ ratios far lower than those of the wallrocks. The quartz samples also show strong positive Eu anomalies with Eu/Eu* ratios being 2.01 and 2.23, respectively, and their $(La/Sm)_N$ ratios are similar to those of the wallrocks.

In consideration of the paragenetic relationship between quartz and sulfides, it is believed that both of them were precipitated from the same fluid. It is noticeable that the contents of ore-forming elements (Cu, Pb, Zn etc.) in quartz from the altered wallrock are also high, suggesting that the formation of ore-forming fluids may be intimately related to the fluids responsible for wallrock alteration.

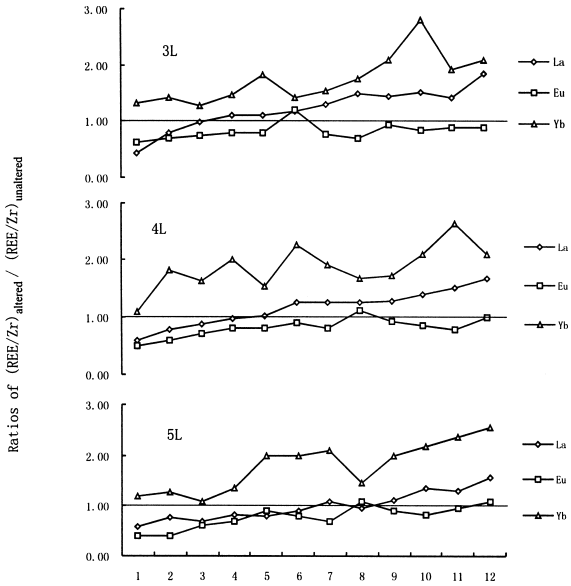

Fig. 6. Variation tendency of $(REE/Zr)_{altered}/(REE/Zr)_{unaltered}$ ratios for the altered phyllites.

DISCUSSION

Mobility of the REE and other trace elements during alteration

A convincing demonstration of trace element mobility must satisfy two criteria (Campbell *et al*., 1984): (1) the range of trace elements concentrations in the rock before and after alteration must be known with confidence; and (2) the absolute abundances and the ratios of the mobile trace elements should vary between altered and unaltered rocks. The point to emphasize is that it is not sufficient to show the absolute abundances of trace elements change before and after alteration, because this can simply result from dilution or concentration if other elements are added to or removed from the rock.

Variations in the absolute abundances of trace elements are described above. Here we discuss the mobility of trace elements by combining the absolute abundances with the ratios of trace element/Zr. Zr was chosen as a denominator because: (1) it was determined to be one of the least mobile elements; (2) it is not geochemically similar to the REE, allowing a comparison of relative mobility of the different REE; and (3) its abundance can be determined with high analytical precision. We calculated the trace element/Zr ratios for the altered and unaltered phyllite on the basis of trace element abundances listed in Tables 1, 2 and 3, but the lists are too long to be presented here. Instead, we discuss the results with some representative unaltered phyllite REE/Zr-normalized ratios illustrated in Fig. 6, where La and Yb rep-

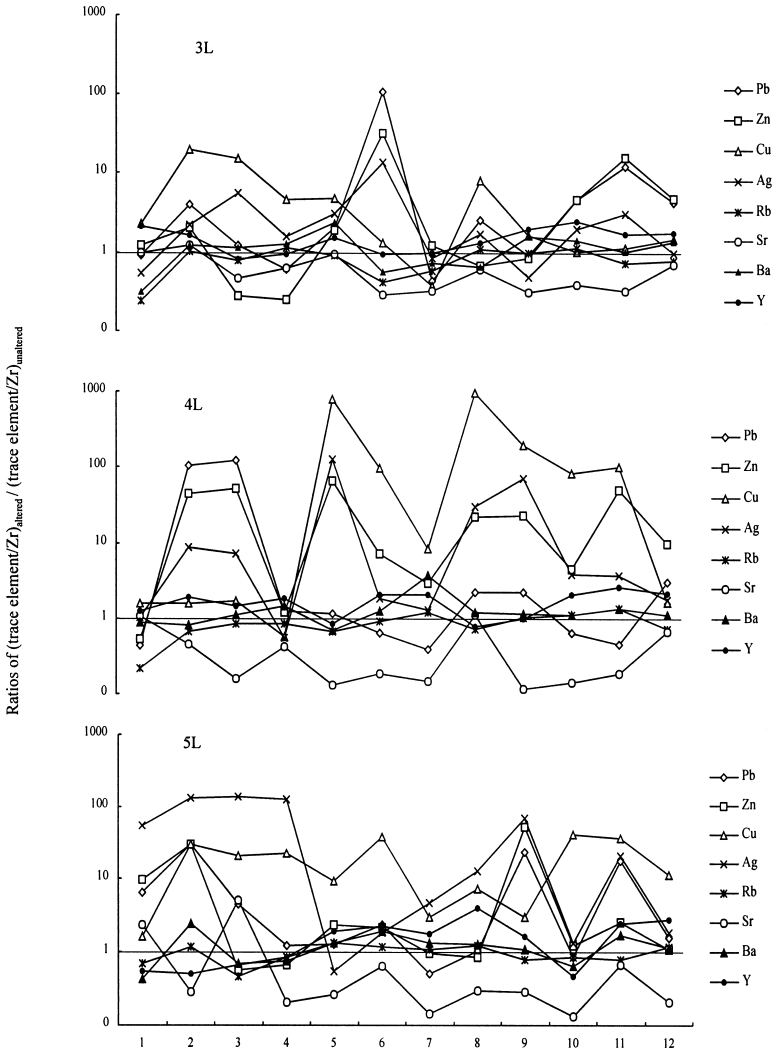

Fig. 7. Variation tendency of (trace element/Zr)$_{altered}$/(trace element/Zr)$_{unaltered}$ ratios for the altered phyllites.

resent for LREE and HREE respectively. And the unaltered phyllite trace element/Zr-normalized ratios are illustrated in Figs. 7 and 8.

The trace element/Zr ratios show quite spectacular evidence of trace elements mobility. LREE/Zr ratios for the altered samples collected from where close to the intrusions on the three levels are lower than that of the unaltered equivalent (appear as the ratios less than unity in Fig. 6), and the greater the depth is, the wider the low-LREE/Zr-ratio zone will be (i.e., 5L > 4L > 3L). On level 5, even some heavy REE (Gd, Tb, Dy, Ho, Er) have lower ratios than that of the unaltered phyllite. This is in consistent with the variation trend of ∑REE as mentioned above. This suggests that the LREE have been systematically lost from the most altered samples, and the higher the degree of alteration (the deeper in depth and the closer to the intrusion), the greater the REE remobilization. On the other hand, HREE show little variable in most of the samples, suggesting the relatively immobility of HREE during hydrothermal alteration.

With increasing distance of the samples from

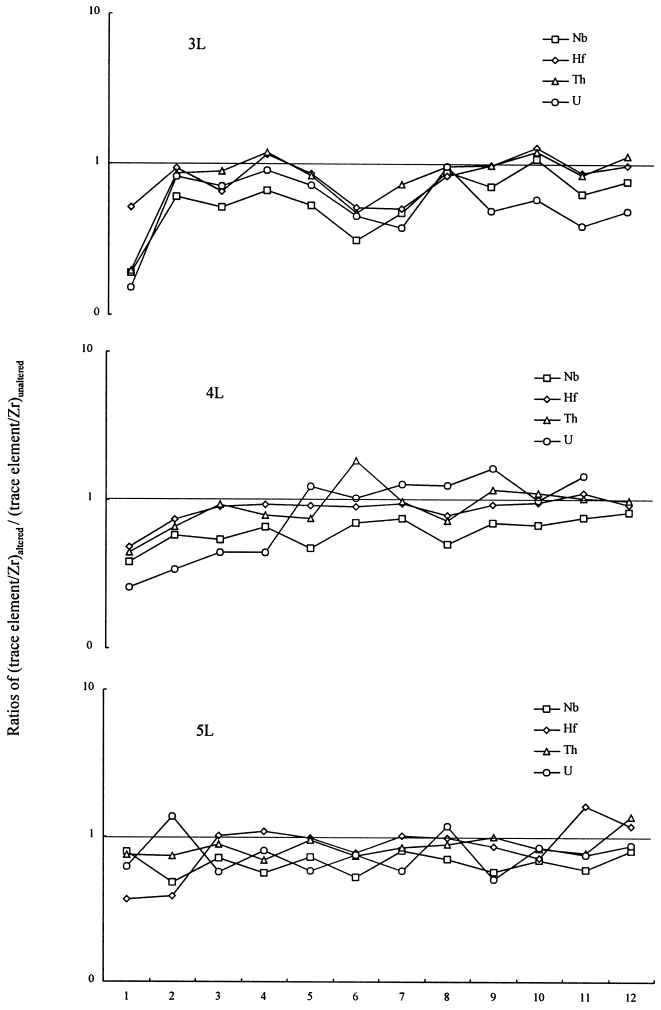

Fig. 8. Variation tendency of (trace element/Zr)$_{altered}$/(trace element/Zr)$_{unaltered}$ ratios for the altered phyllites.

the intrusions, both of LREE/Zr and HREE/Zr ratios increase and all are greater than that of the unaltered phyllite, indicating that the REE in fluids tend to be precipitated in the altered rocks when they are transported outwards.

Eu/Zr ratios are lower than that of the unaltered phyllite in almost all of altered samples, suggesting that Eu is pervasively leached during hydrothermal alteration. And there is a tendency of intensifying leaching process close to the intrusions. This can be explained by the properties of Eu and the related fluids that will be discussed in the following section.

Summarily, the overall depletion in REE abundances in samples from where close to the intrusions may be attributed to two factors: (1) loss of REE, especially LREE and Eu from the rocks during hydrothermal alteration. (2) dilution with silica added to the altered rocks by silicification during hydrothermal alteration. The enrichment of REE in samples from where far away from the intrusions is probably due to the addition of REE from hydrothermal solutions to the altered phyllite by the unloading of REE in response to the drop of temperature during the REE were transported outwards by fluids.

Trace element/Zr ratios for LILE (Fig. 7) such as Rb and Sr remain little variable, while Ba is significantly changed, suggesting the immobility of Rb and Sr, and the mobility of Ba during hydrothermal alteration. Rb is dominantly hosted by K-bearing minerals, which in the phyllites in the Yinshan deposit is dominated by sericite. Since sericite could only experience recrystallization during hydrothermal alteration that would not change the chemical composition significantly, Rb would not be released from the sericite. Sr is generally considered to present in plagioclase by replacing Ca, but in the present study little or no plagioclase has been found in phyllite of Yinshan deposit. So the form and state of Sr remain unknown. The significantly enrichment of Ba can be explained by the barite observed in the altered phyllite that also reported by previous investigators (Jiangxi G.E.B., 1996). It is thus clear that the LILE in this deposit show quite different behaviors due to the different fates of the host minerals during hydrothermal alteration. This is different from what was reported by some studies in which Rb, Sr and Ba were simultaneously mobilized (Campbell *et al.*, 1984 and references therein).

Nb/Zr, Hf/Zr, Th/Zr, and U/Zr ratios are remarkably similar between the altered and unaltered phyllites (Fig. 8), suggesting that these elements remain relatively immobile during hydrothermal alteration.

Y/Zr ratios (Fig. 7) generally show no evidence of mobile, excepting for some samples, indicating that Y behavior similar to those of the HREE.

The trace element/Zr ratios of ore-forming elements (Fig. 7) such as Pb, Zn, Ag and Cu are remarkably increased in the altered phyllites, suggesting that hydrothermal solutions introduced these elements. However, the irregularity of spatial distribution for the ore-forming elements suggest that the processes of fluid transport and unloading of the elements are very complicated, i.e., the complex superimposition of multi-episode and multi-stage hydrothermal alteration, hydrothermal transport path as well as the mechanism of unloading of ore-forming materials.

REE characteristics and properties of hydrothermal solutions

Quartz possesses a very stable skeleton of crystal structure and hence the REE could by no means be incorporated into its lattice (Liu *et al*., 1984). Rossman *et al*. (1987) and Norman *et al*. (1989) deduced that the REE in quartz might be hosted predominantly in its fluid inclusions. In their studies, Su *et al*. (1998) provided strong evidence for the above deduction. Therefore the REE characteristics of quartz can reflect those of the fluid from which they were precipitated.

Two forms of quartz can be recognized from the altered phyllite in the Yinshan deposit: one coexits with sulfides in the orebodies and its REE characteristics can reflect those of ore-forming fluid, and the other is the ore-barren quartz veins occurring in the altered phyllites, which is the product of hydrothermal alteration and can mirror the REE characteristics of hydrothermal solutions responsible for hydrothermal alteration in the area studied. As mentioned above, quartz in the orebodies and that in ore-barren quartz veins are both characterized by low $\sum$REE, strong positive Eu anomaly, lower $(La/Yb)_N$ than, and similar $(La/Sm)_N$ to those of the wallrocks. These kinds of quartz show much similarity in REE characteristics, implying probably that they have genetic connections.

Moreover, the contents of ore-forming elements in the altered phyllites are significantly increased, implying the genetic connections between hydrothermal solutions involved in alteration and ore-forming fluids. It is deduced from inclusion characteristics and the hydrogen and oxygen isotope data (Zhang and Liu, 1999) that the ore-forming fluids and the fluids responsible for the alteration of phyllites were partly derived from the same source.

By comprehensive study on inclusion, Lin and He (1993) concluded that ore-forming fluids for the Yinshan deposit are a kind of slightly acidic (pH = 4–5.37, averaging 4.87), strongly reductive fluids (Eh = –1.12 eV)—both the values of pH and Eh were obtained by calculation on the basis of inclusions' chemical compositions. In terms of

the theoretical studies by Bau (1990), under similar conditions to the ore-forming fluids in the Yinshan deposit, Eu would be present in the more mobile form of Eu^{2+} in the fluids. In their studies, Campbell *et al*. (1984) find that Eu^{2+} is more mobile than Eu^{3+} and also more mobile than the other tri-valence REE. Therefore the authors deduce that hydrothermal alteration in the Yinshan deposit removed Eu from the altered phyllites, producing greater negative Eu anomalies in the rocks. And the removed Eu was finally precipitated in the ore-barren quartz veins in the wallrocks.

The possible REE-hosting minerals in the phyllites

In the present study, no REE-enriched minerals such as apatite, zircon, rutile etc. could be observed by detailed microscopic analyses for the altered phyllites. Furthermore, artificially panning studies on the samples in combination with X-ray diffraction analysis indicated that the main panning-concentrate minerals in the phyllites are pyrite and galena. Again, REE-enriched minerals such as apatite, zircon and rutile could not be identified. This suggests that those REE-enriched minerals would be very low in amounts and thus could not become the main REE-hosted minerals in phyllites in the Yinshan deposit. Moreover, the minor mineral quartz in the phyllites has been known has to no affinity for the REE. Therefore, we deduced that the dominant mineral of the phyllites (sericite) is probably the main REE-hosted mineral. Roaldset (1975) reported that: (1) In the case of the existence of REE-riched minerals such as apatite, zircon and rutile, the contents of REE in micas and other phyllosilicates would be extremely low, indicating the poor affinity of the REE for the crystal structures of micas and other phyllosilicates; and (2) In case of the absence of more REE selective minerals, the REE contents of micas and other phyllosilicates are very high. However, most of the REE in mica was extractable by rinsing with EDTA (ethylenediamine tetra-acetic acid, which is a chemical agent that does not attack the phyllosilicates minerals to such an extent that noticeable changes occur in the X-ray diffractograms after the samples to be treated), with the maximum up to 90%. This suggests that the REE do not enter the lattice of the minerals and occupy the cation positions. Instead, they are adsorbed on the surfaces of exchangeable cations of the crystal structure layers (tetrahedral and octahedral layers). Terakado and Fujitani (1998) also deduced that the REE in the Roseki deposit might be present among the structured layers of phyllosilicates. So we deduce that the REE in phyllites of the Yinshan deposit may be present mainly among the structure layers of sericite.

Clues provided by REE and trace element characteristics to metallogenesis

Characteristics of the major elements and REE in altered phyllites from the main geological profile of the Yinshan deposit clearly show that: $3^{\#}$ and $13^{\#}$ intrusions are the center of hydrothermal alteration and mineralization. The fluids causing wallrock alteration are genetically connected with the ore-forming fluids. Meanwhile, the characteristics of the major elements and REE in the wallrocks of the three representative orebodies suggest that the locations where the orebodies appear might be small centers of the heat and fluid sources. As mentioned above, the contents of ore-forming elements in the altered phyllite are significantly increased. This fact, in conjunction with isotope studies by previous investigators (Jiangxi G.E.B., 1996) and on the basis of the data that silica of quartz in the orebodies and that of ore-barren quartz veins were found their sources in the wallrocks, suggests that parts of the ore-forming fluids were a circulated strata water which descended to the depth, mixed up with hydrothermal solutions derived from magma and evolved into the ore-forming fluids, then found their way upwards through the fault system to the locus of ore deposition. The ore-forming fluids can also cause hydrothermal alteration in the wallrock of orebodies. The larger the orebodies, the stronger the wallrock alteration will be. And then more remarkable leaching-loss and “dilution” of REE will be seen in the samples from where close to the orebodies. This suggests that the REE character-

istics for the altered country rocks of the orebodies in the Yinshan deposit have a close bearing on the size of orebodies. Studies by Whitford *et al*. (1988), Ganzeyev *et al*. (1987) and Arvanitidis and Richard (1986) also revealed that the degree of REE mobility in the wallrocks increased with the sizes of massive Cu-Zn sulfide deposits. This suggests that those prospective for metal mineralization might have a distinctive REE signature and, therefore, the REE may have some applications for exploration. For the case in the Yinshan deposit, the degree of REE diluted by REE-barren minerals (quartz and sulfides) and lost by hydrothermal alteration is probably an effective geochemical indicator for distinguishing between small and large orebodies at the later stage of exploration, a possibility that requires further testing by investigation of more orebodies.

CONCLUSIONS

(1) REE, especially LREE, were selectively leached from the Shuangqioashan Group phyllites that had been undergone dominantly recrystallization of the major minerals during hydrothermal alteration. The greater the degree of alteration, the stronger the remobilization of REE. LREE were leached from the rocks close to the intrusions and then were redeposited in the part far away from the intrusions. It led to the observed much stronger negative Eu anomalies in the altered phyllites that Eu was systematically leached from the rocks.

(2) The lower total REE in the samples from where close to the intrusions than those from where far away from the intrusions is probably attributed to two factors. One is the dilution of REE-barren minerals (quartz and sulfides), and the other is leaching out of REE from the rocks by hydrothermal alteration.

(3) REE in the hydrothermal solutions are characterized by enrichment in LREE, strong positive Eu anomalies and much smaller $(La/Yb)_N$ ratios than those of the phyllites. The addition of REE from the hydrothermal solutions resulted in smaller $(La/Yb)_N$ ratios in the altered phyllites than that of the unaltered equivalent.

(4) For other trace elements, Y behaved similarly to HREE. The LIL elements such as Rb, Sr and Ba behaved differently which may be attributed to the different fates of their main hosting minerals. The ore-forming elements such as Cu, Pb, Zn, Ag and Sn were remarkably added to the altered phyllites, while Hf, Th, U, Nb, and Zr remained rather constantly during hydrothermal alteration.

(5) It is suggested by the REE features that ore-forming fluids probably found their ways upwards from the depth through faults to the locus of ore deposition, where to be small centers of hydrothermal alteration.

(6) The degree of REE mobility increases with the sizes of the orebodies. Thus, REE is probably an effective geochemical indicator for distinguishing between small and large orebodies at the later stage of exploration, however, this viewpoint require further testing by investigation to more orebodies.

Acknowledgments—The authors wish to thank all the personnel of the Section of Geological Survey of the Yinshan Mining Administration, especially Senior Engineers Zhang Jingzhang and Liu Shengxiang for their great support during field work. Thanks are due to Prof. Qiu Yuzuo for carefully reviewing the manuscript (in Chinese) as well as for his constructive modification and suggestions. We also thank Drs. Y. Terakado, K. Yamamoto and an anonymous reviewer for their critical and constructive reviews that helped to improve the manuscript. This work was financially supported by the National Science Foundation of China through the project 49625304 and by the Ministry of Science and Technology of China through a national Climbing Project 95-p-39.

REFERENCES

Arvanitidis, N. D. and Richard, D. T. (1986) An evaluation of lanthanide geochemistry in ore petrology. *Miner. Wealth* **46**, 21–28.

Bau, M. (1990) Rare-earth mobility during hydrothermal and metamorphic fluid-rock interaction and the significance of the oxidation state of europium. *Chem. Geol*. **93**, 219–230.

Boulvais, P., Fourcade, S., Moine, B., Gerard, G. and Cuney, M. (2000) Rare-earth elements distribution

in granulite-facies marbles: a witness of fluid-rock interaction. *Lithos* **53**, 117–126.

Campbell, I. H., Lesher, C. M., Coad, P., Franklin, J. M., Gorton, M. P. and Thurston, P. C. (1984) Rare-earth elementmobility in alteration pipes below massive Cu-Zn-sulfide deposits. *Chem. Geol*. **45**, 181–202.

Ganzeyev, A. A., Sotskav, Y. P. and Lyapunov, S. M. (1987) Geochemical specialization of ore-bearing solutions in relation to rare-earth elements. *Geochem. Int*. **20**, 160–164.

Giuliani, G., Chelletz, A. and Mechiche, M. (1987) Behavior of REE during thermal metamorphism and hydrothermal infiltration associated with skarn- and vein-type tungsten orebodies in Central Morocco. *Chem. Geol*. **64**, 279–294.

Jiangxi, G. E. B. (1996) *Yinshan Cu-Pb-Zn-Au-Ag Deposit in Jiangxi G.E.B. Province*. Geological Publishing House, Bejing, 105–334 (in Chinese).

Lin, D.-S. and He, G.-C. (1993) A study of fluid inclusions of mineral in Yinshan deposit in Jiangxi. *Mineral Resources and Geology* **3**, 50–58 (in Chinese).

Ling, Q.-C. and Liu, C.-Q. (2001) Behavior of rare-earth elements in fluid-rock interaction: A review. *Acta Mineralogica Sinca* **4**, 80–90 (in Chinese with English abstract).

Liu, Y.-J., Cao, L.-M. and Li, Z.-L. (1984) *Elements Geochemistry*. The Publishing House of Science, Beijing, 6–215.

Matthews, S. J., Marguillas, R. A., Kemp, A. J., Grange, F. K. and Gardeweg, M. C. (1996) Active skarn formation beneath Lascar Volcano, northern Chile: a petrographic and geochemical study of xenoliths in eruption products. *J. Metam. Geol*. **14**, 509–530.

Norman, D. I., Kyle, P. R. and Baron, C. (1989) Analysis of trace elements including rare earth elements in fluid inclusion liquid. *Econ. Geol*. **84**, 162–166.

Pan, Z.-L., Zhao, Ai.-X. and Pan, T.-H. (1993) *Mineralogy*. Geological Publishing House, Beijing, 56–87.

Panteley, A. (1986) A Canadian cordilleran model for epithermal gold-silver deposits. *Gesci. Cana*. **13**, 101–111.

Qi, L., Hu, J. and Gregoire, D. C. (2000) Determination of trace elements in granites by inductively coupled plasma mass spectrometry. *Talanta* **51**, 507–513.

Roaldset, E. (1975) Rare-earth element distribution in some precambriam rocks and their phyllosillicates, Numedal, Norway. *Geochim. Cosmochim. Acta* **39**, 455–469.

Rossman, G. R., Wei's, D. and Wasserburg, G. J. (1987) Rb, Sr, Nd and Sm concentration in quartz. *Geochim. Cosmochim. Acta* **51**, 2325–2329.

Su, W.-C., Qi, L. and Hu, R.-Zh. (1998) Determination of rare earth elements in fluid inclusions by ICP-MS. *Chinese Science Bulletin, 1998* **43**(10), 1094–1098.

Terakado, T. and Fujitani, T. (1998) Behavior of the rare earth elements and other trace elements during interactions between acidic hydrothermal solutions and silicic volcanic rocks, southwestern Japan. *Geochim. Cosmochim. Acta* **62**(11), 1903–1917.

Vander Auwera, J. and Andre, L. (1991) Trace elements (REE) and isotopes (oxygen, carbon, strontium) to characterize the metasomatic fluid sources from the skarn deposit (iron, tungsten, copper) of Traversella (Ivrea, Italy). *Contrib. Mineral. Petrol*. **106**, 325–339.

Whitford, D. J., Korsch, M. J., Porritt, P. M. and Craven, S. J. (1988) Rare-earth element mobility around the volcanogenic polymetallic massive sulfide deposits at Que River, Tasmania, Australia. *Chem. Geol*. **68**, 105–119.

Whitney, P. R. and Olmsted, J. F. (1998) Rare earth element metasomatism in hydrothermal systems: The Willsboro-Lewis wollastonite ores, New York, USA. *Geochim. Cosmochim. Acta* **62**, 2965–2977.

Zhang, D.-H. (1997) On several questions of ore-forming processes in the Yinshan polymetallic deposit. *Geological review* **43**(5), 490–497 (in Chinese with English abstract).

Zhang, D.-H. and Liu, W. (1999) Research on Fluid Inclusions of the Yinshan Polymetallic Deposit, Jiangxi G.E.B. Province, China. *Chinese Journal of Geochemistry* **18**(2), 104–114.